Supplementary Information

Photo-responsive lignin fragment-based polymers as switchable adhesives

Pallabi Sinha Roy,[a,b] Matthieu M. Mention,[c] Antonio F. Patti,[a,b] Gil Garnier,*[b,c] Florent Allais*†[b,c] and Kei Saito*†[d]

[a.] School of Chemistry, Monash University, Clayton VIC 3800, Australia. [b.] Department of Chemical Engineering, Bioresources Processing Research Institute of Australia (BioPRIA), Monash University, Clayton VIC 3800, Australia. [c.] URD Agro-Biotechnologies Industrielles (ABI), CEBB, AgroParisTech, 51110, Pomacle, France. [d.] Graduate School of Advanced Integrated Studies in Human Survivability, Kyoto University, Higashi-Ichijo-Kan, Yoshida-nakaadachicho 1, Sakyo-ku, Kyoto, 606-8306, Japan, † K. Saito and F. Allais contributed equally to this work.

Table of Contents

1. ^{1}H and ^{13}C NMR spectra of the synthesized monomers

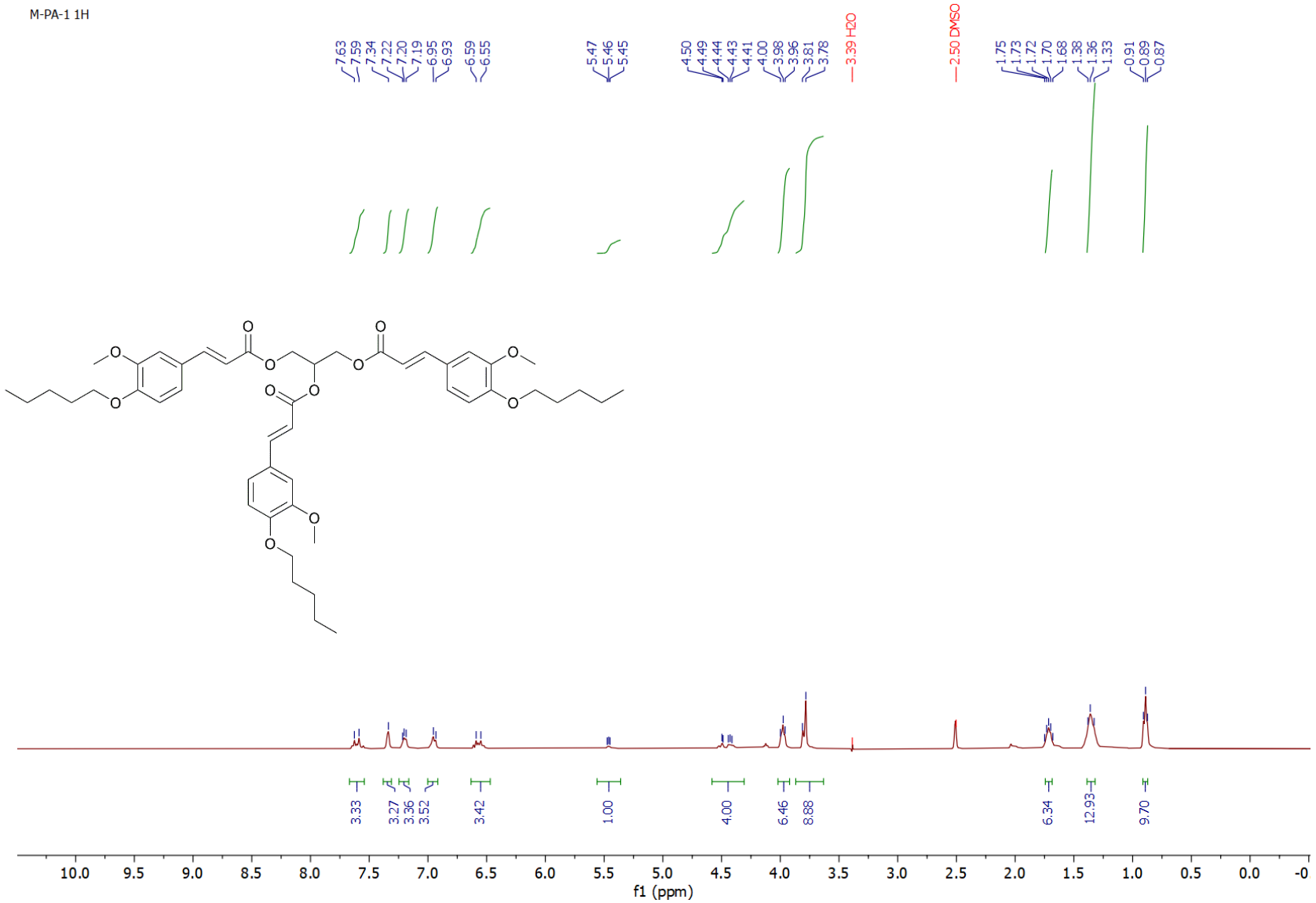

Figure S1. ^{1}H NMR spectrum of M-PA-1 in DMSO-d_6.

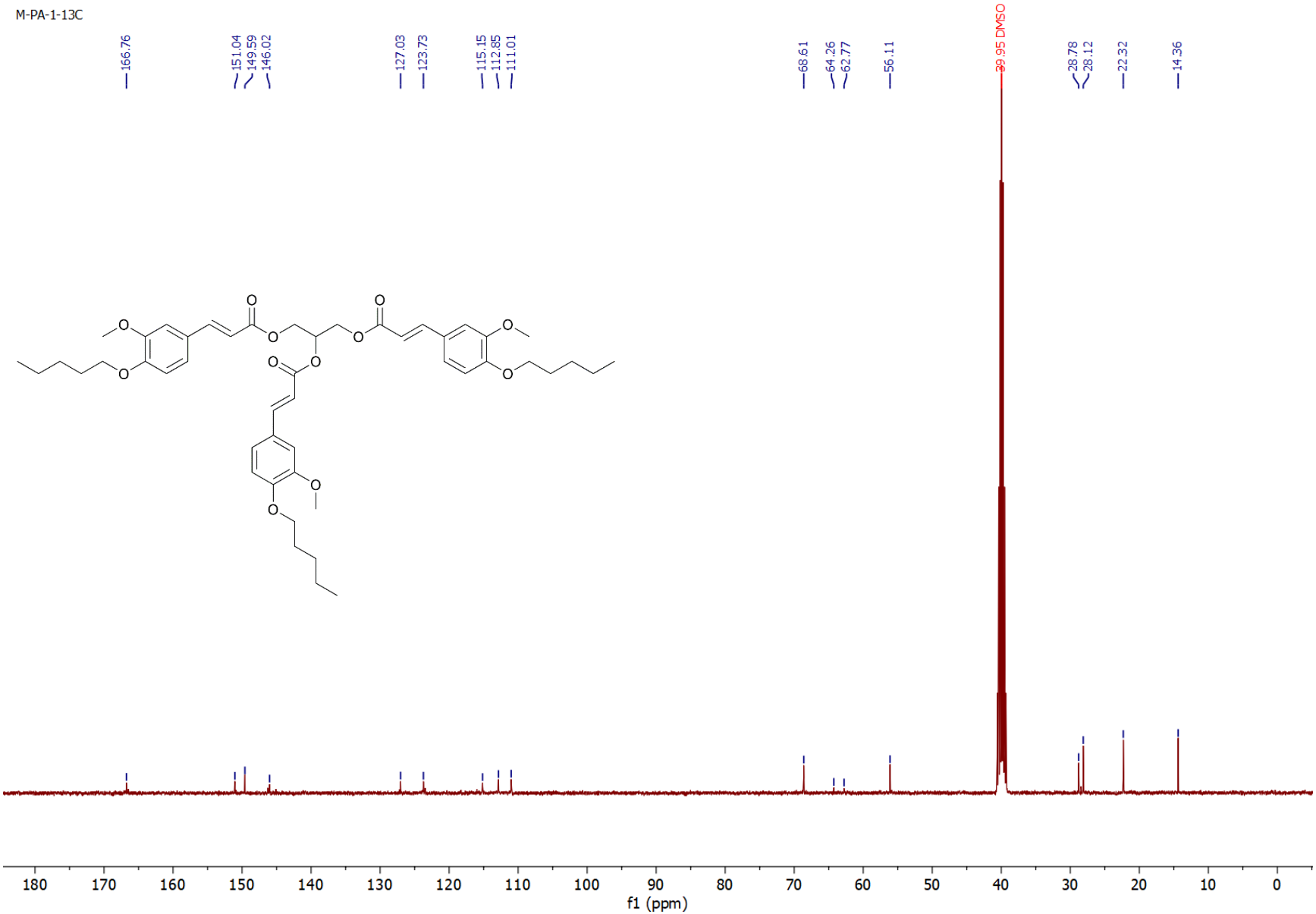
M-PA-1-13C
166.76
151.04
149.59
146.02
127.03
123.73
115.15
112.85
111.01
68.61
64.26
62.77
56.11
39.95 DMSO
28.78
28.12
22.32
14.36
180
170
160
150
140
130
120
110
100
90
80
70
60
50
40
30
20
10
0
f1 (ppm)

Figure S2. ^{13}C NMR spectrum of M-PA-1 in DMSO-d_6.

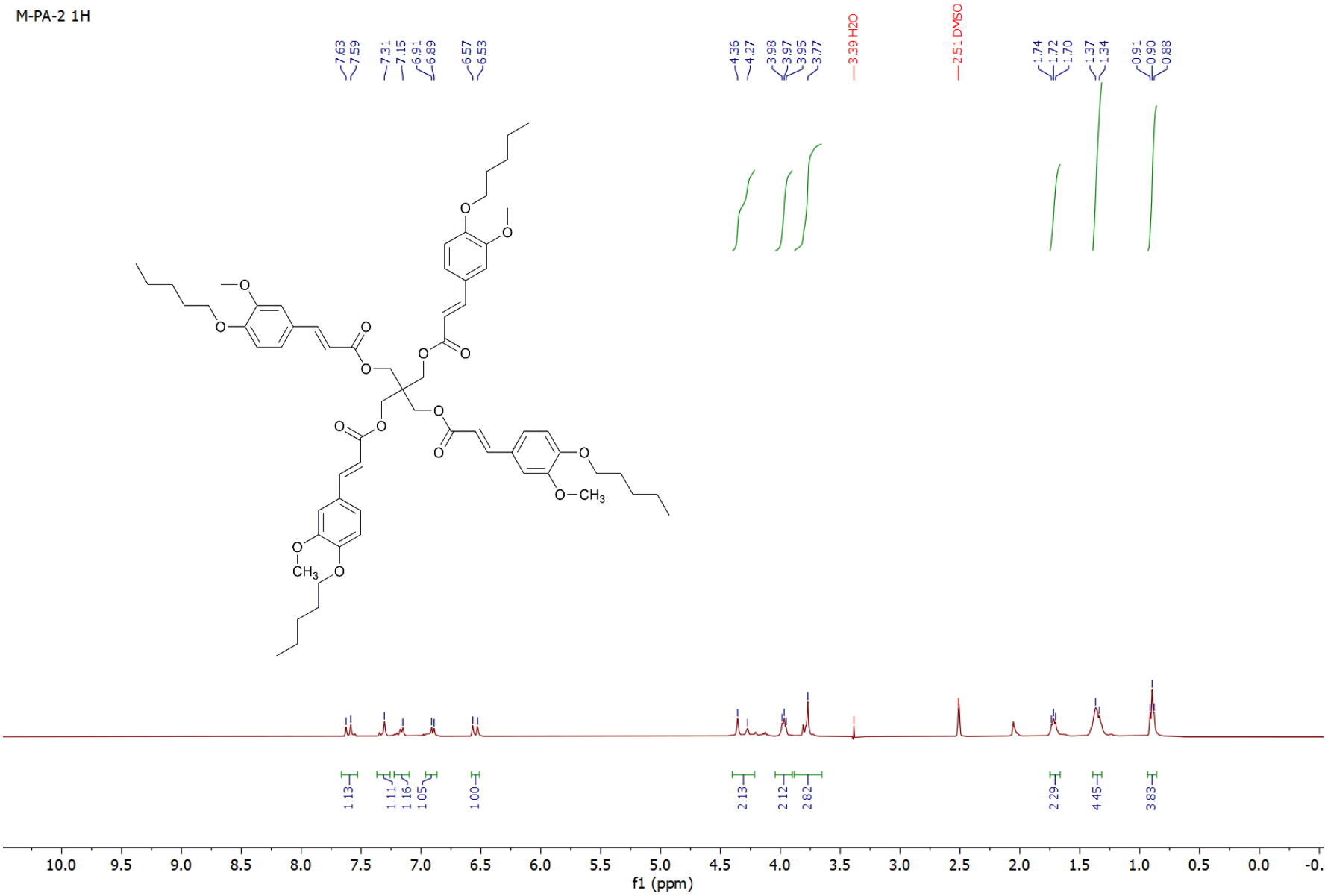

Figure S3. ^{1}H NMR spectrum of M-PA-2 in DMSO-d_6.

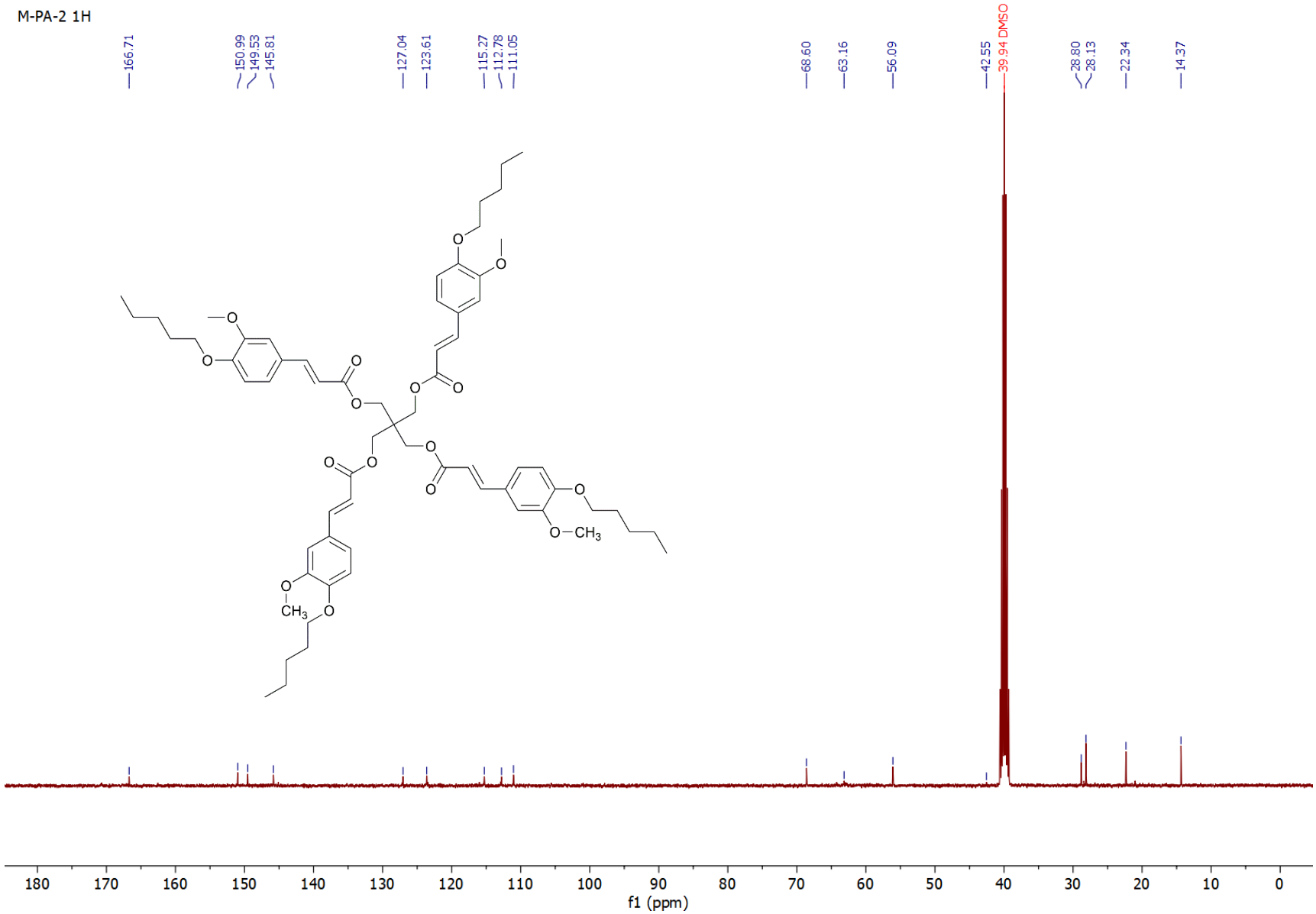

Figure S4. ^{13}C NMR spectrum of M-PA-2 in DMSO-d_6.

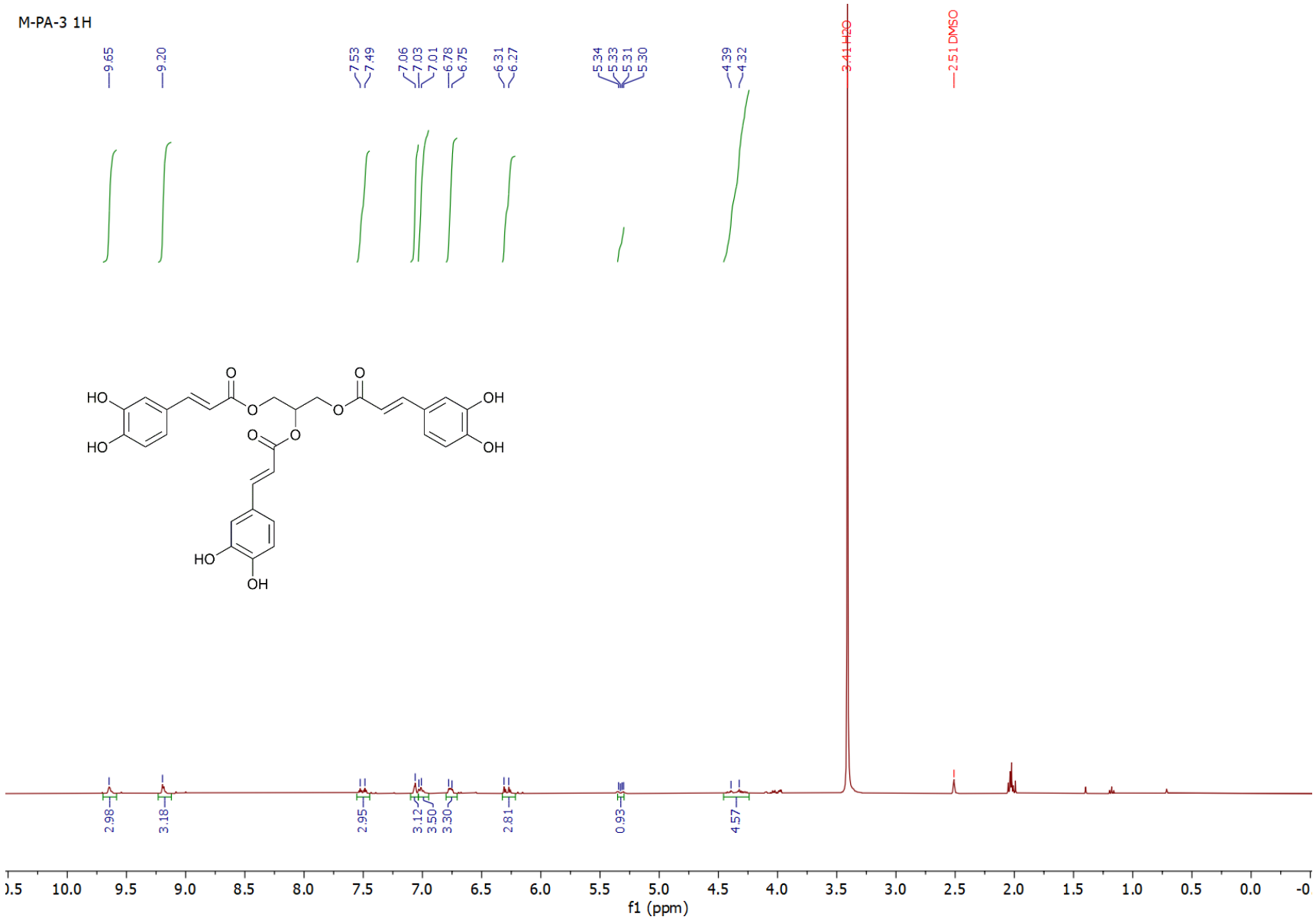

Figure S5. ^{1}H NMR spectrum of M-PA-3 in DMSO-d_6.

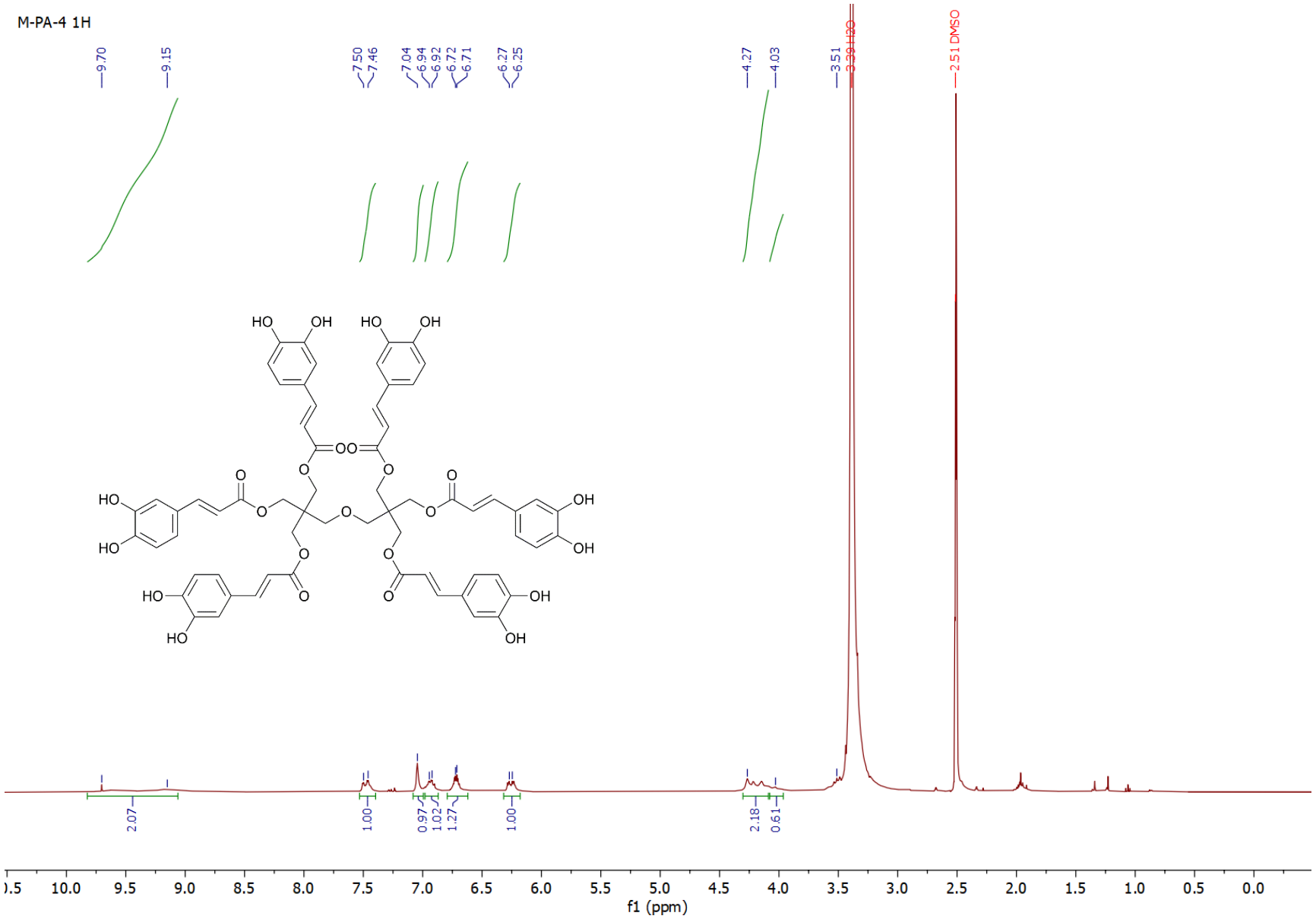
M-PA-4 1H
9.70
9.15
7.50
7.46
7.04
6.94
6.92
6.72
6.71
6.27
6.25
4.27
4.03
3.51
3.39 H2O
2.51 DMSO
HO
OH
O
2.07
1.00
0.97
1.02
1.27
1.00
2.18
0.61
f1 (ppm)

Figure S6. ^{1}H NMR spectrum of M-PA-4 in DMSO-d_6.

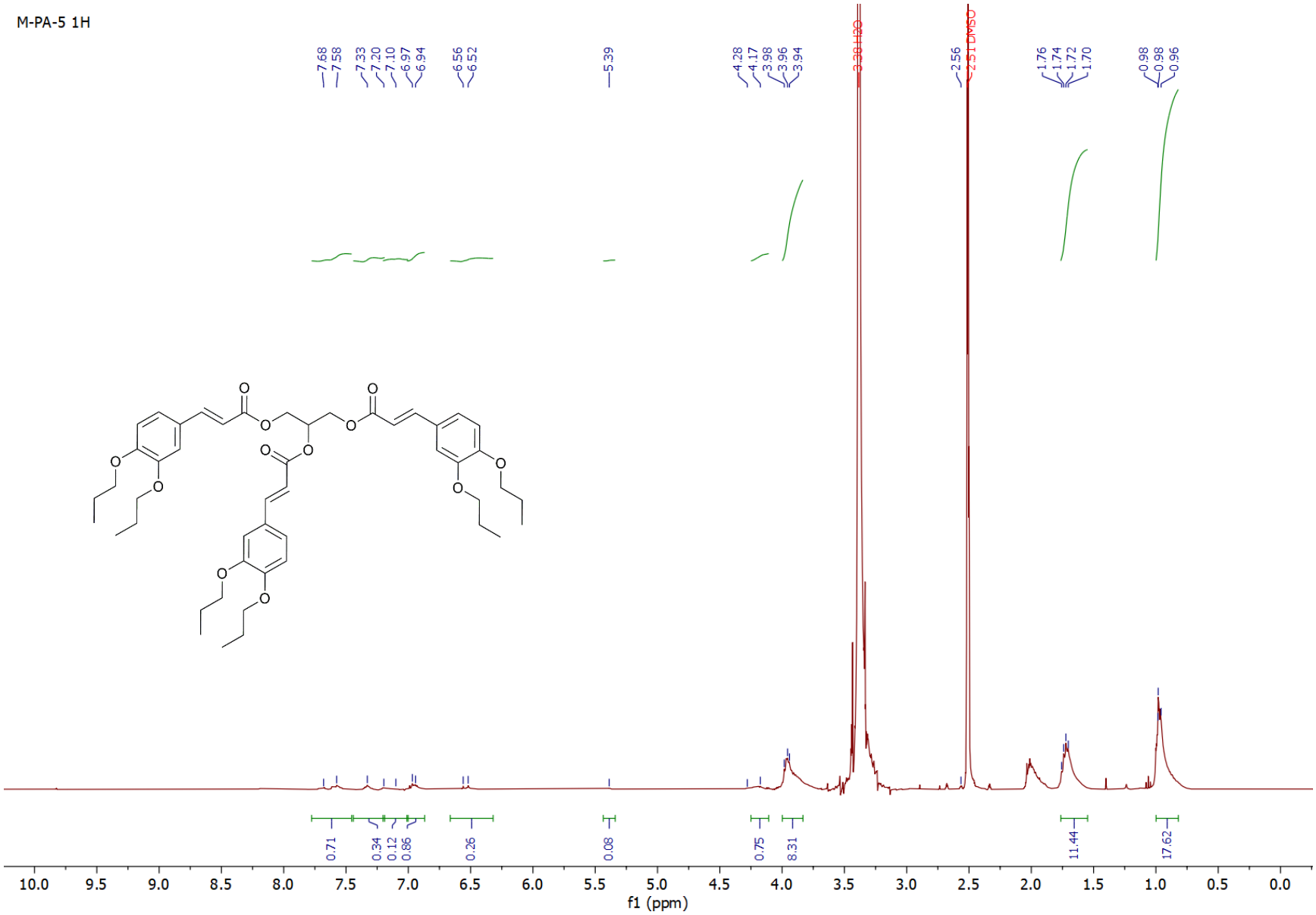

Figure S7. ^{1}H NMR spectrum of M-PA-5 in DMSO-d_6.

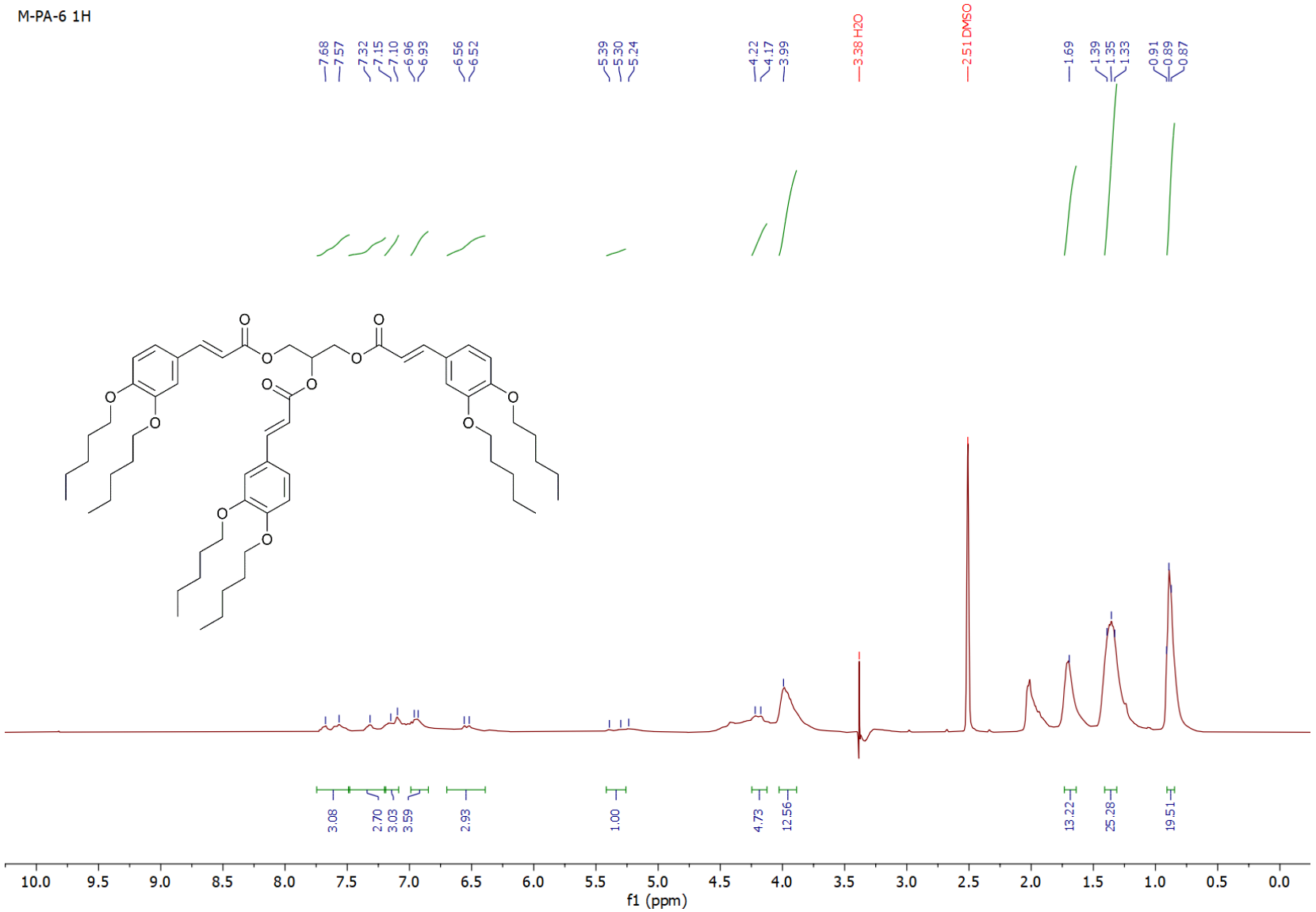

Figure S8. ^{1}H NMR spectrum of M-PA-6 in DMSO-d_6.

2. Comparison of FTIR spectra for compound PA-1 before crosslinking and at crosslinked and decrosslinked state

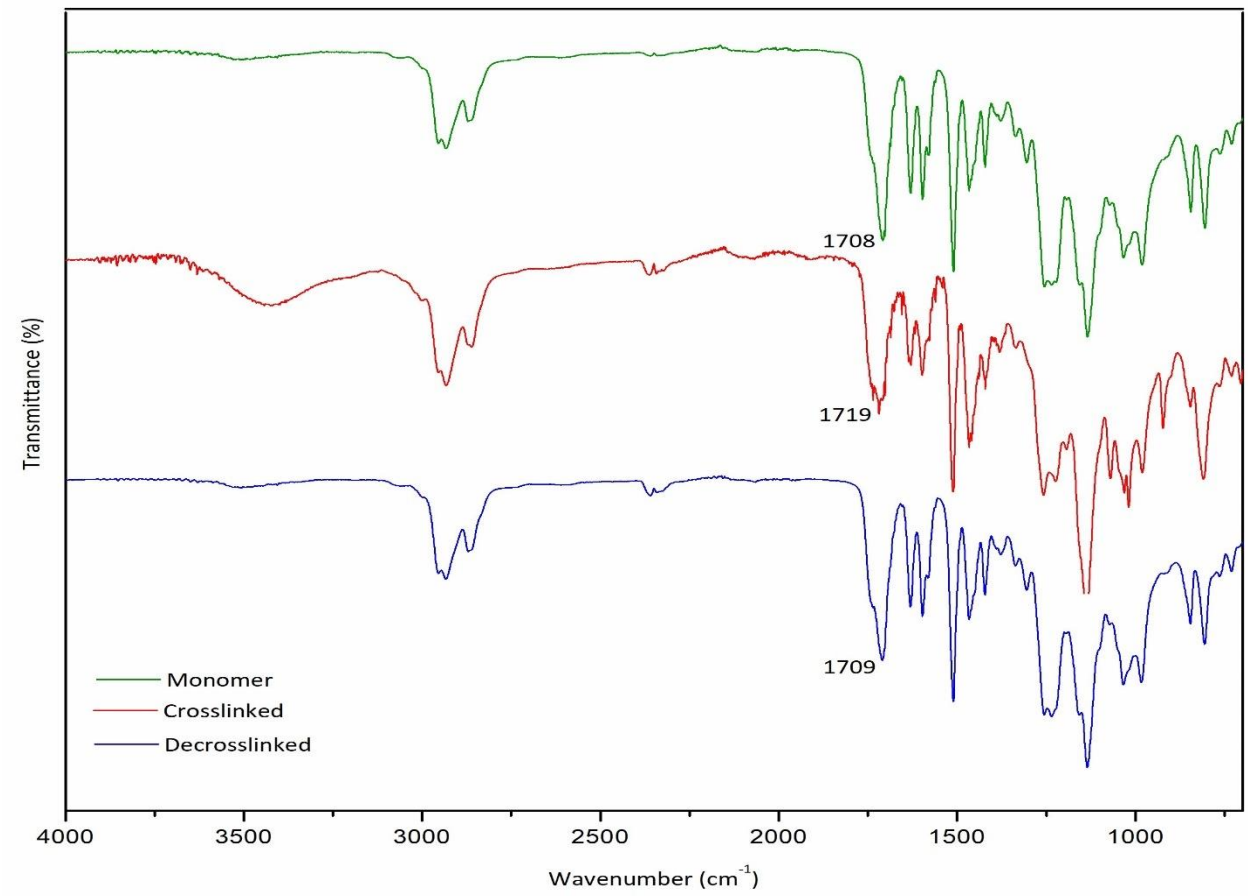

Figure S9. FTIR spectra for PA-1 at monomer, crosslinked and decrosslinked state.

3. UV-Vis spectra for crosslinking and decrosslinking of compounds PA-1 to PA-6

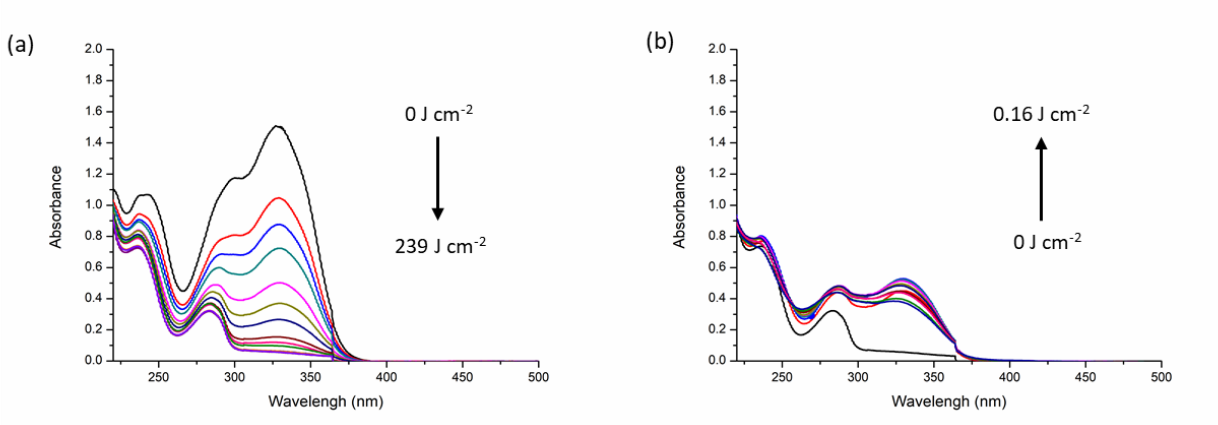

Figure S10. UV-Vis spectra for PA-1. (a) Crosslinking at 365 nm (96%). (b) Decrosslinking at 254 nm (35%).

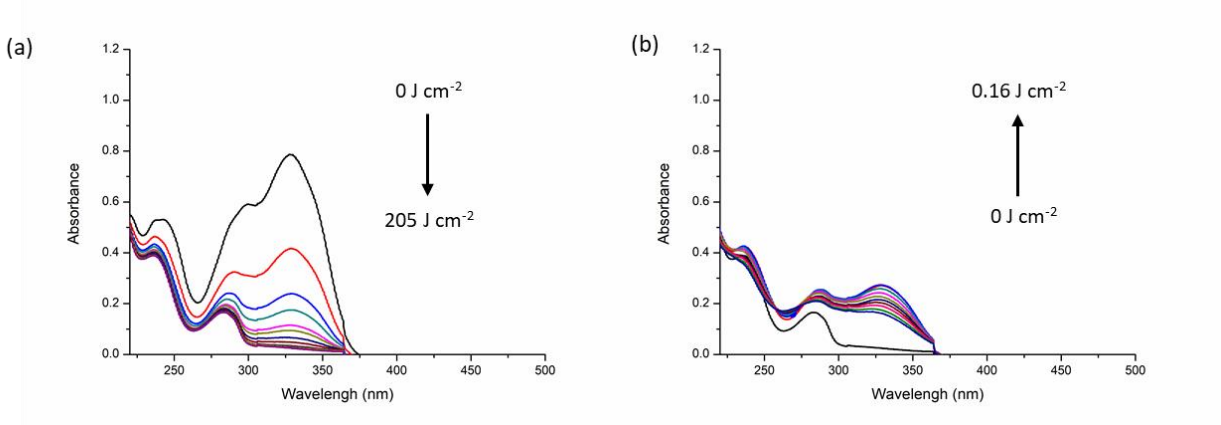

Figure S11. UV-Vis spectra for PA-2. (a) Crosslinking at 365 nm (97%). (b) Decrosslinking at 254 nm (35%).

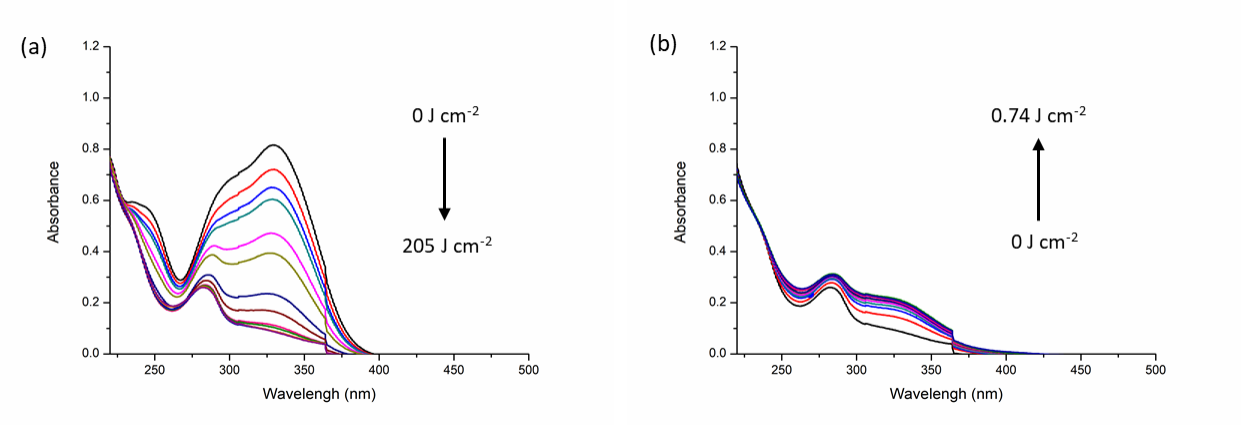

Figure S12. UV-Vis spectra for PA-3. (a) Crosslinking at 365 nm (89%). (b) Decrosslinking at 254 nm (24%).

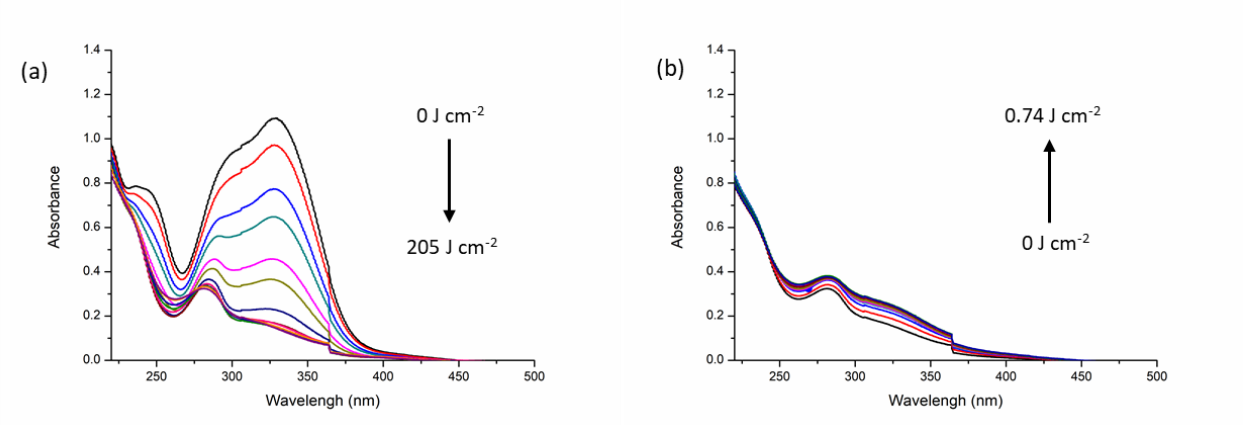

Figure S13. UV-Vis spectra for PA-4. (a) Crosslinking at 365 nm (87%). (b) Decrosslinking at 254 nm (22%).

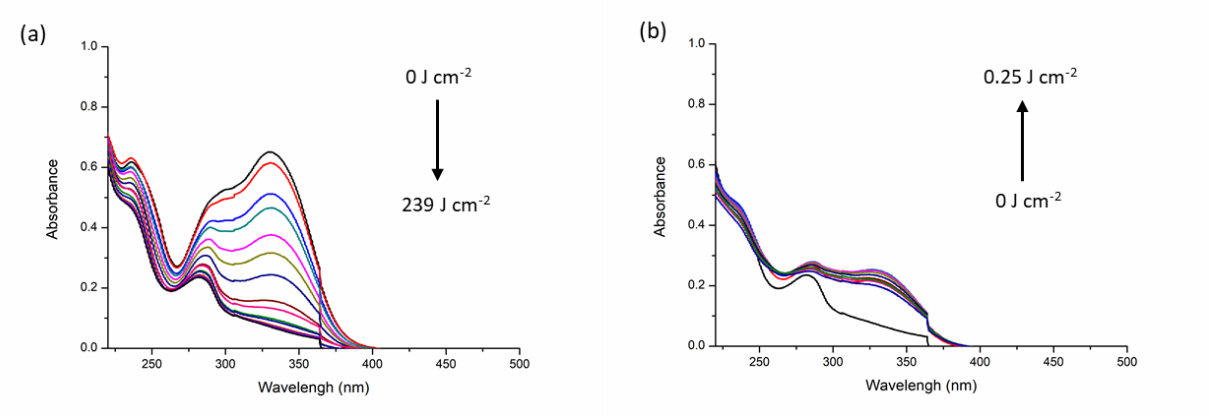

Figure S14. UV-Vis spectra for PA-5. (a) Crosslinking at 365 nm (89%). (b) Decrosslinking at 254 nm (39%).

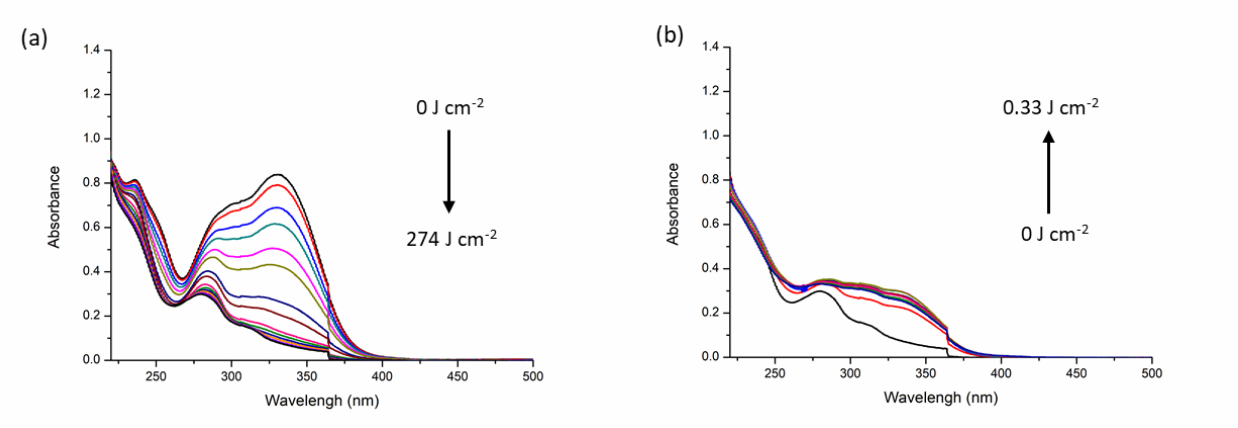

Figure S15. UV-Vis spectra for PA-6. (a) Crosslinking at 365 nm (90%). (b) Decrosslinking at 254 nm (36%).

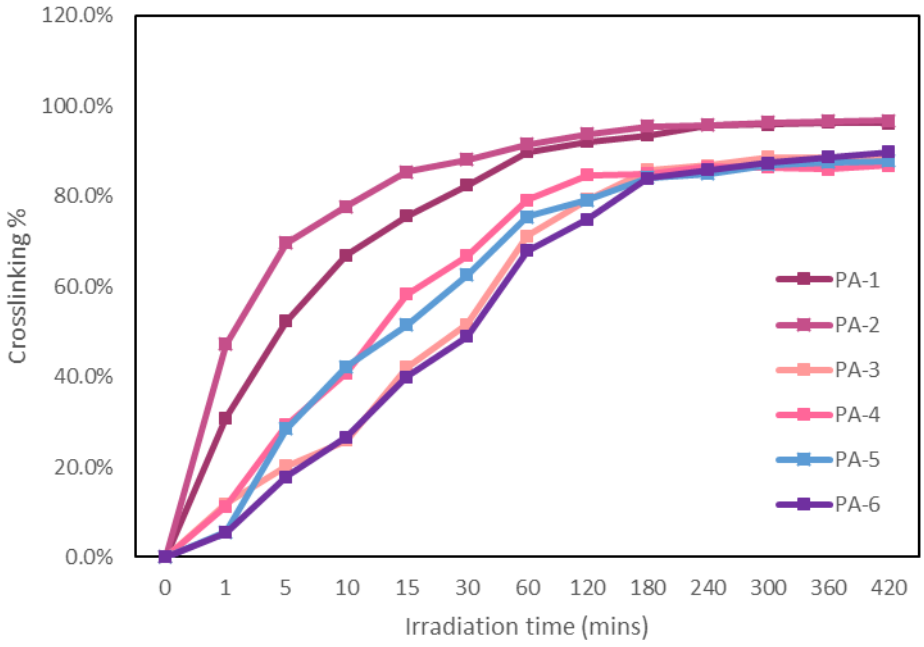

Figure S16. Crosslinking % calculated using UV-Vis spectra for PA-1 to PA-6 with respect to 365 nm irradiation time.

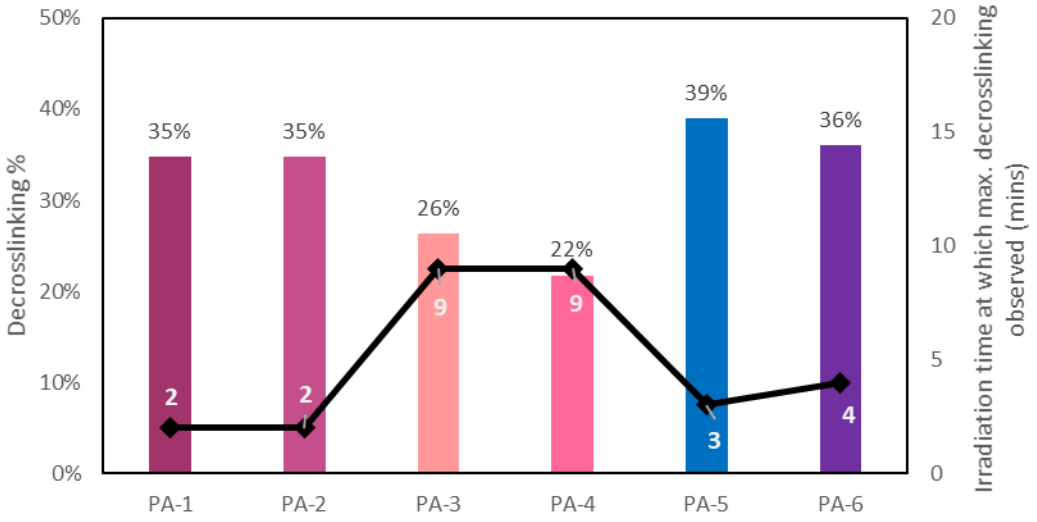

Figure S17. Comparison of decrosslinking % calculated using UV-Vis spectra and the 254 nm irradiation time at which maximum decrosslinking observed for PA-1 to PA-6.

4. Thermogravimetric analysis (TGA) data of polymer adhesive PA-1 to PA-6

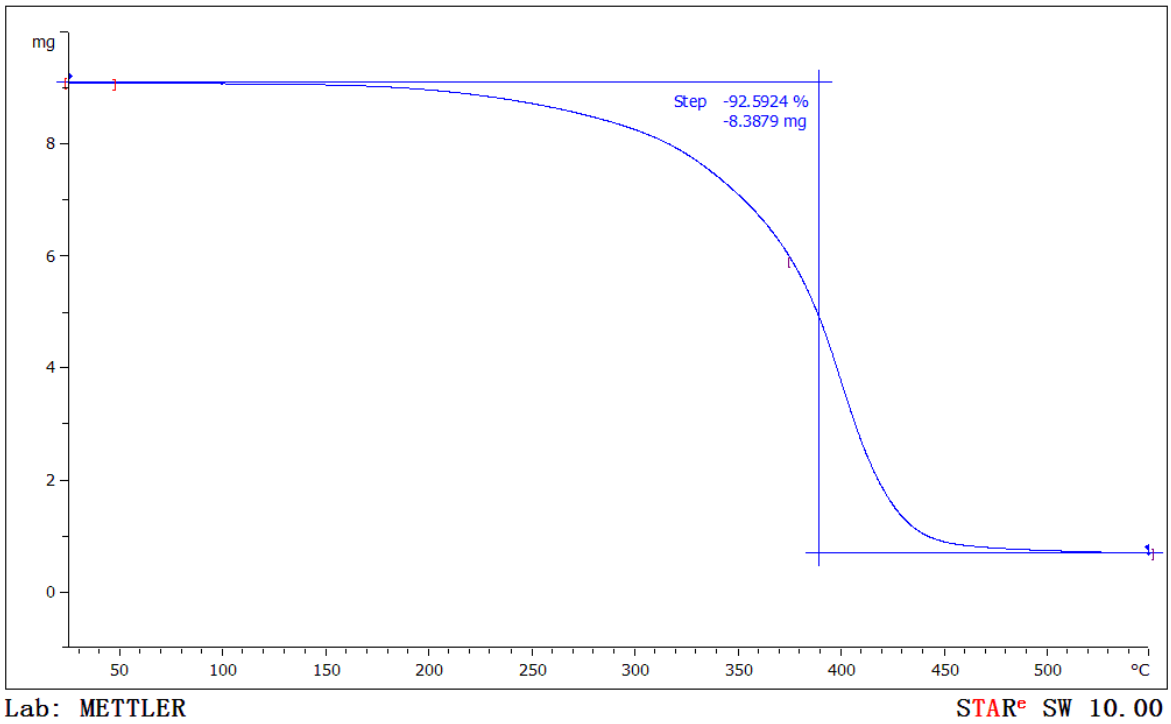

Figure S18. Thermogravimetric analysis data for polymer adhesive PA-1.

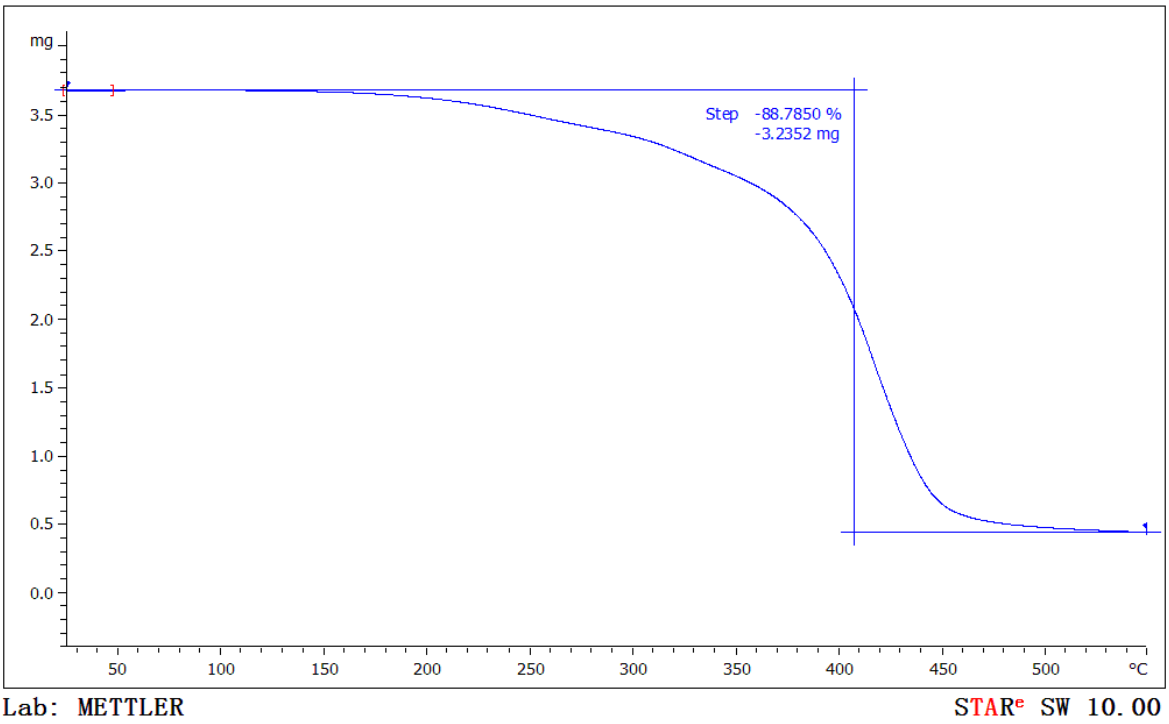

Figure S19. Thermogravimetric analysis data for polymer adhesive PA-2.

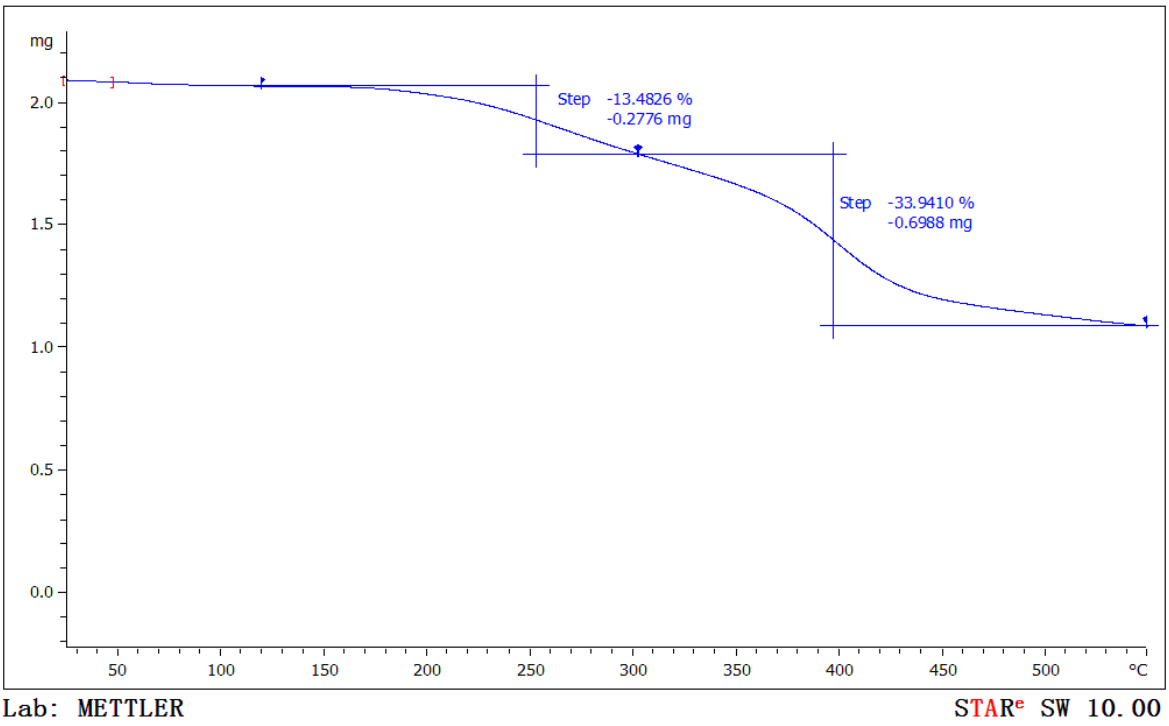

Figure S20. Thermogravimetric analysis data for polymer adhesive PA-3.

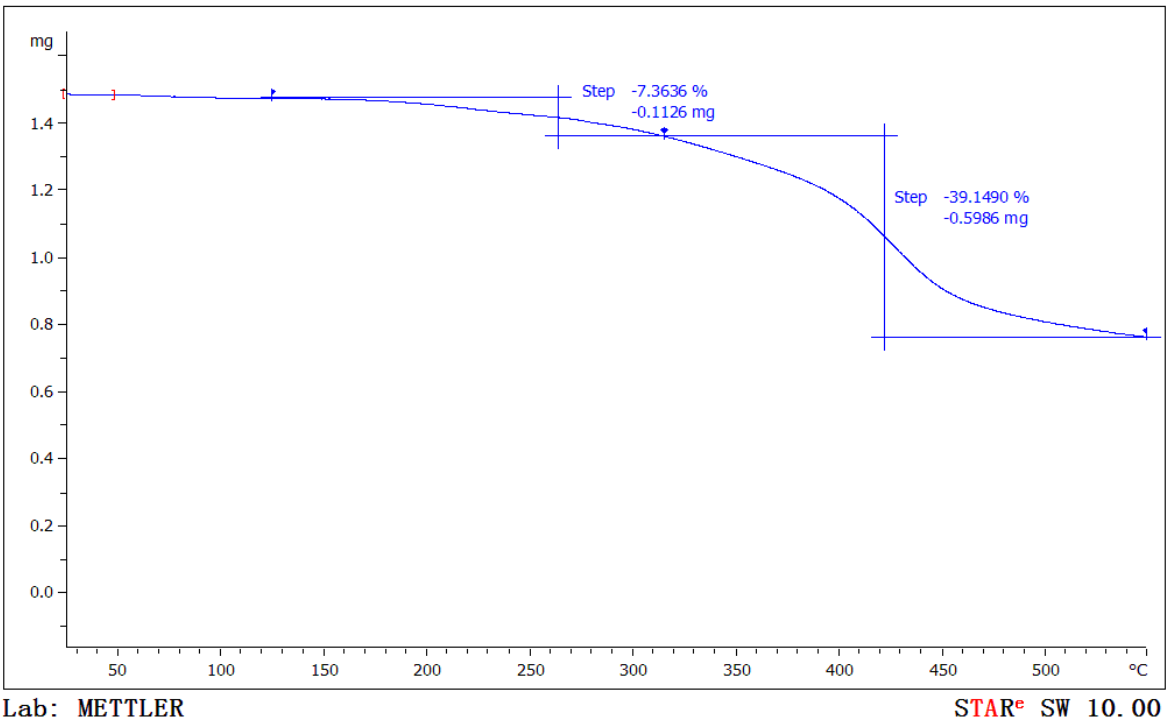

Figure S21. Thermogravimetric analysis data for polymer adhesive PA-4.

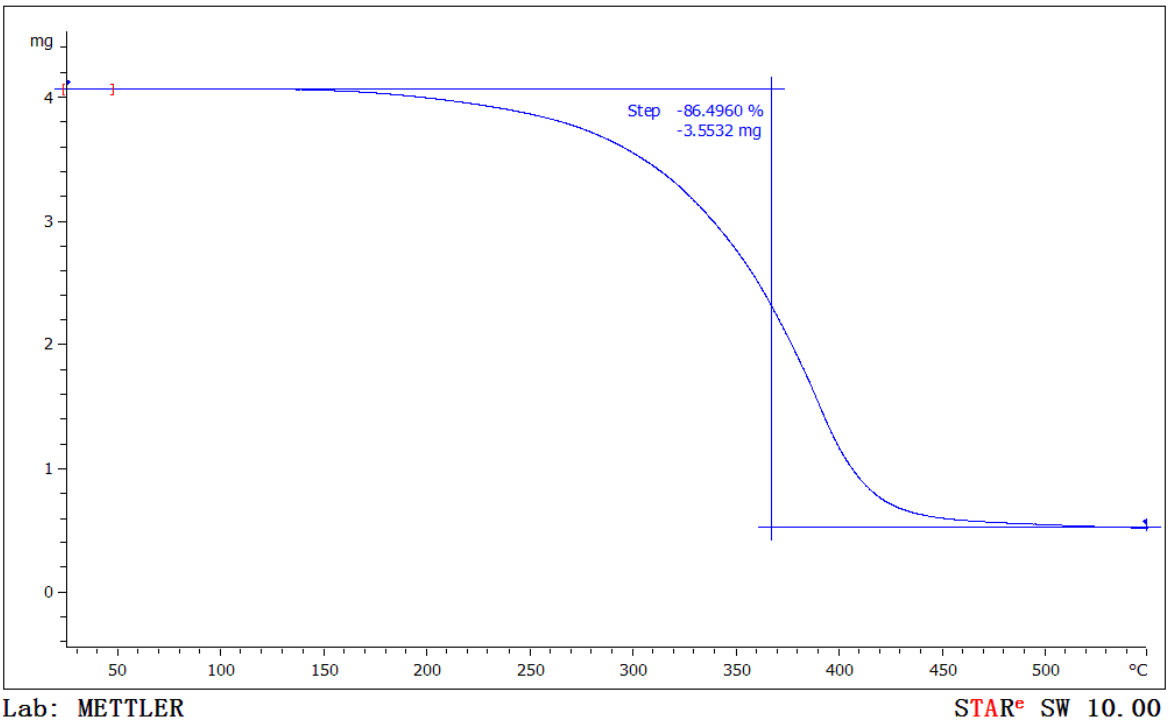

Figure S22. Thermogravimetric analysis data for polymer adhesive PA-5.

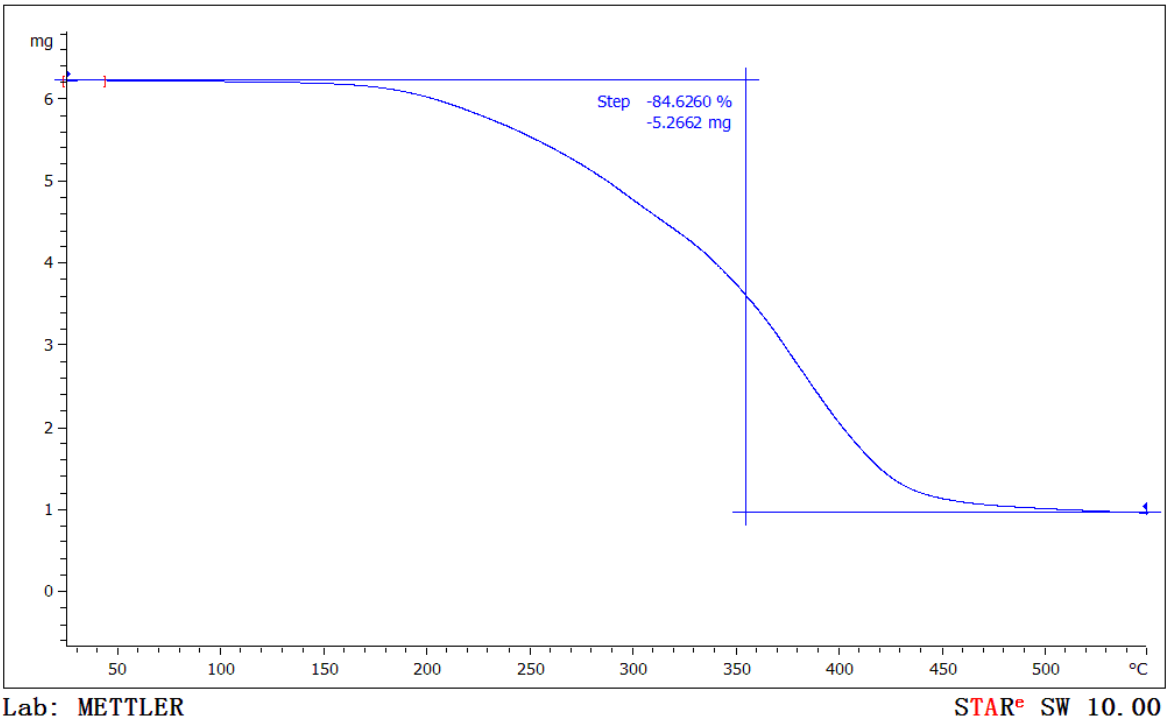

Figure S23. Thermogravimetric analysis data for polymer adhesive PA-6.

5. Glass transition temperature of polymer adhesive PA-1 to PA-6

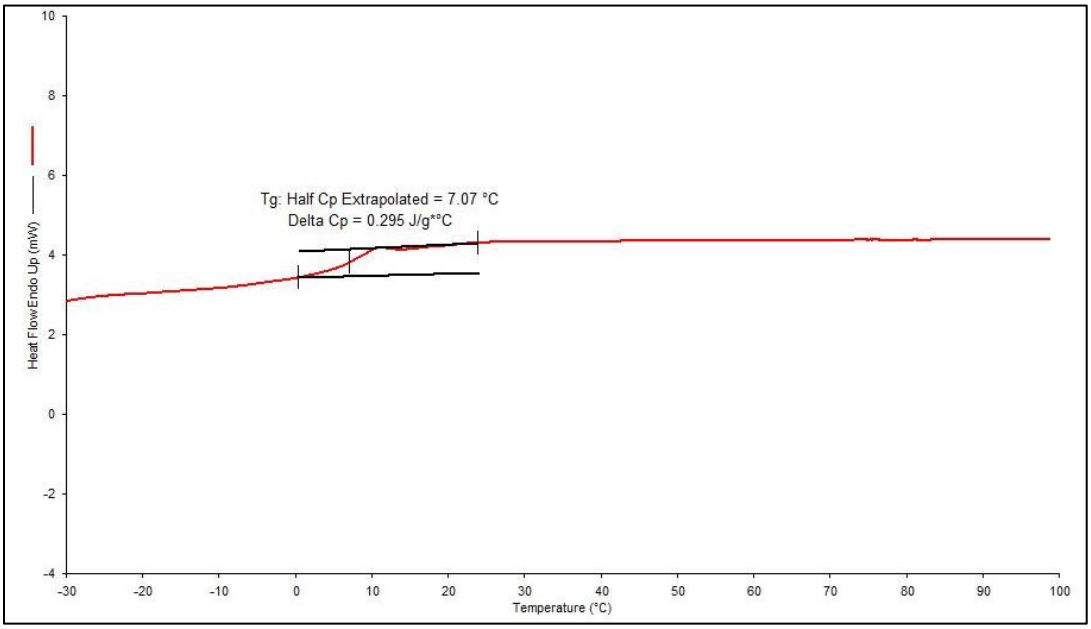

Figure S24. Glass transition temperature for polymer adhesive PA-1 at crosslinked state.

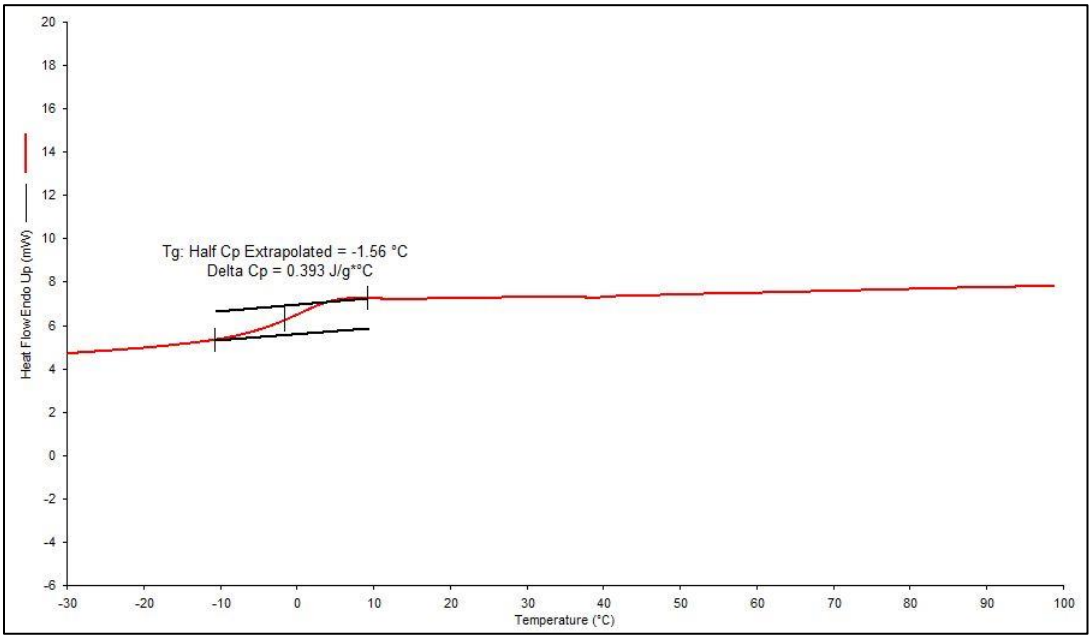

Figure S25. Glass transition temperature for polymer adhesive PA-1 at decrosslinked state.

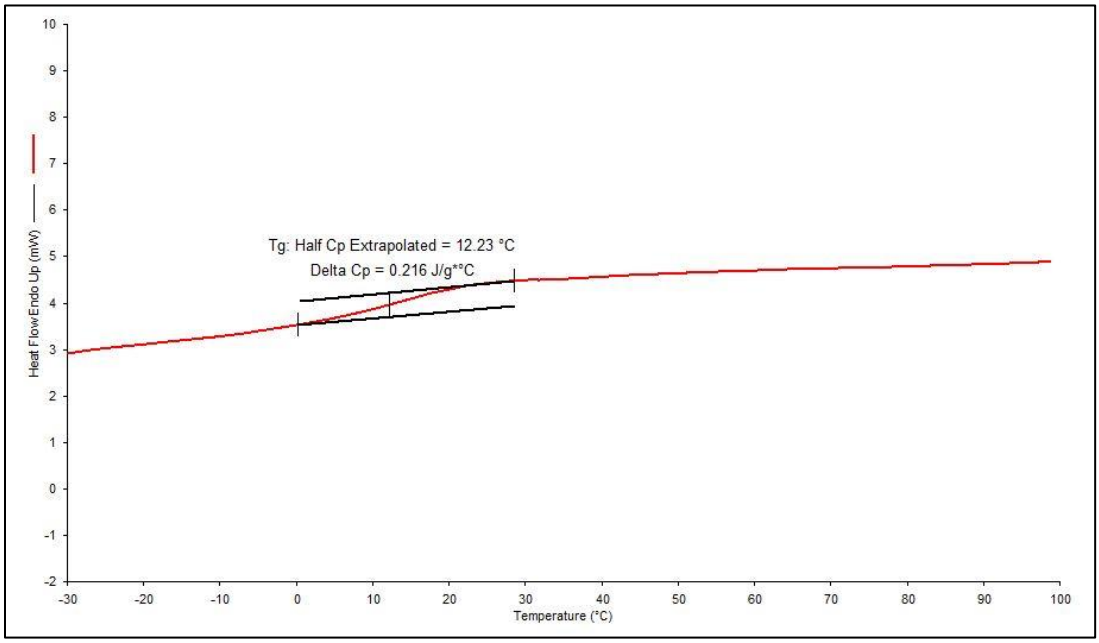

Figure S26. Glass transition temperature for polymer adhesive PA-2 at crosslinked state.

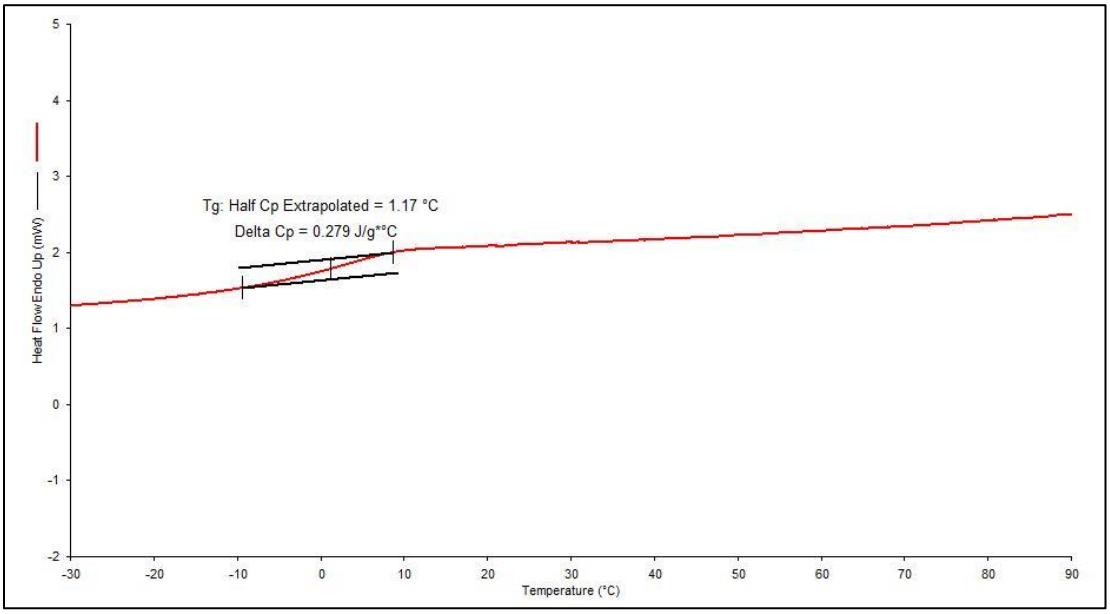

Figure S27. Glass transition temperature for polymer adhesive PA-2 at decrosslinked state.

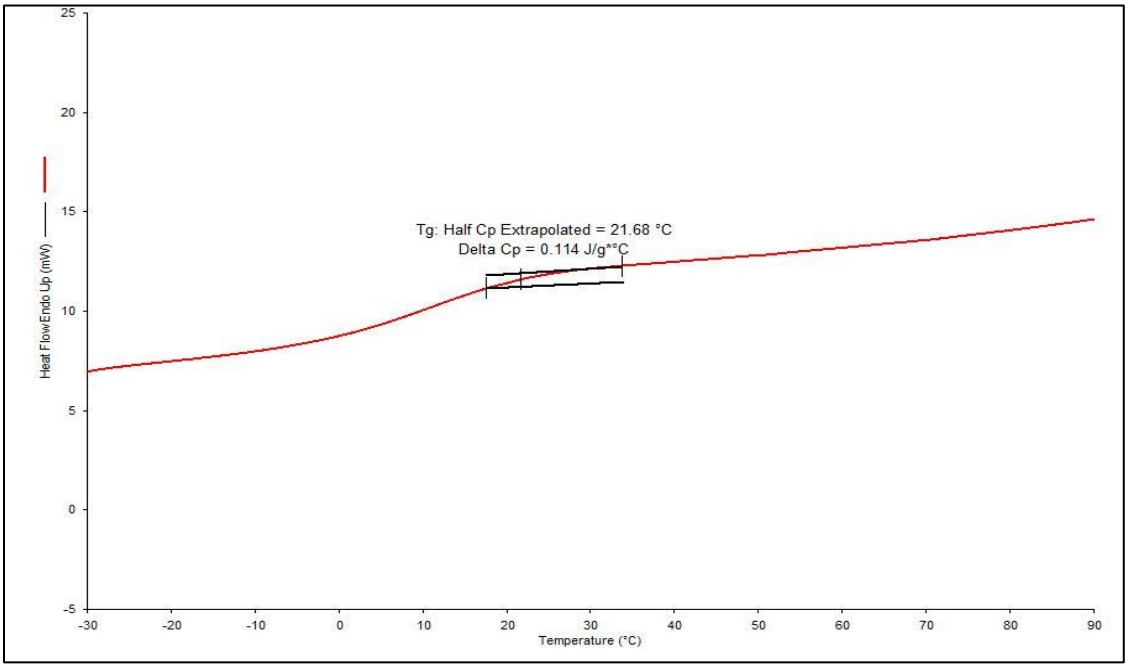

Figure S28. Glass transition temperature for polymer adhesive PA-3 at crosslinked state.

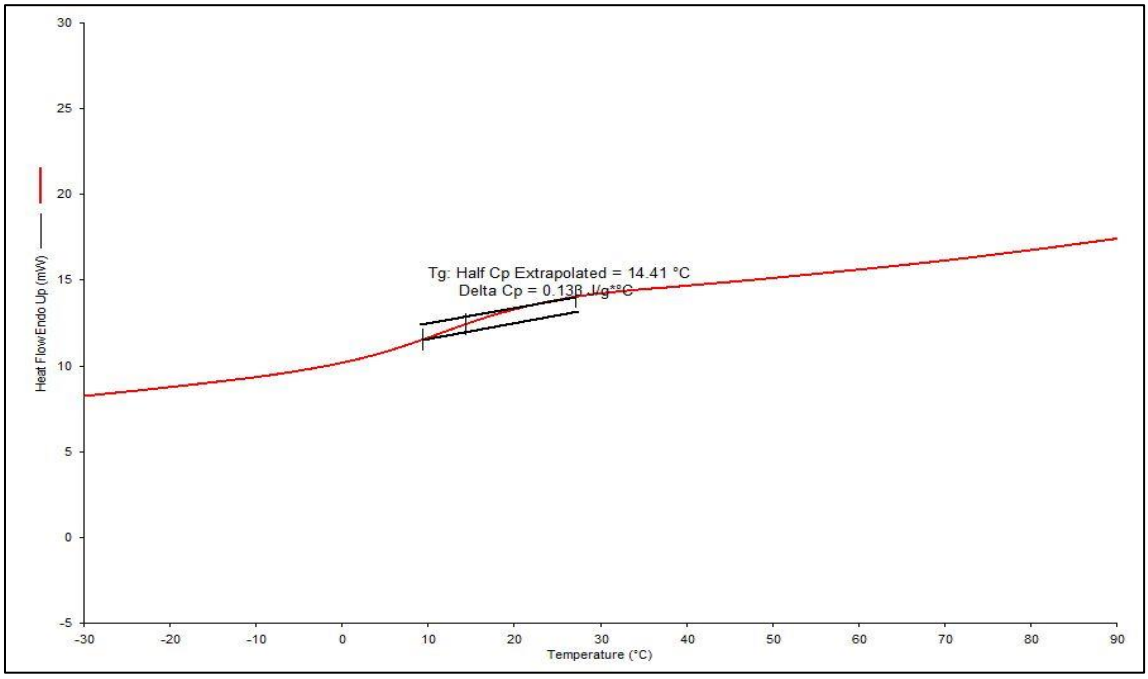

Figure S29. Glass transition temperature for polymer adhesive PA-3 at decrosslinked state.

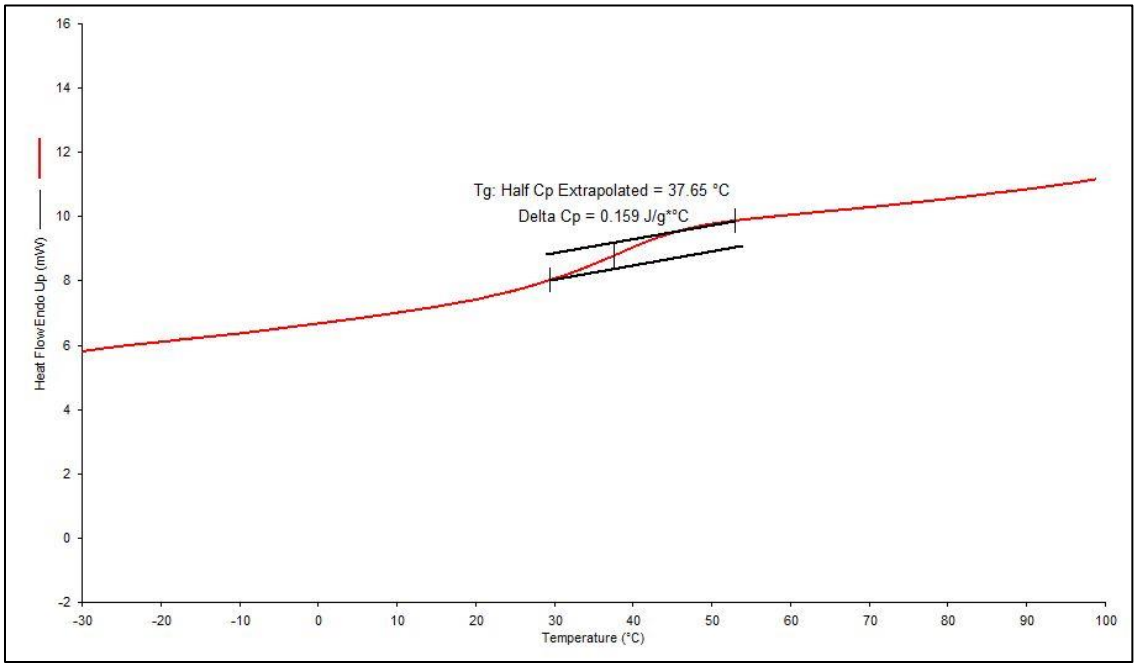

Figure S30. Glass transition temperature for polymer adhesive PA-4 at crosslinked state.

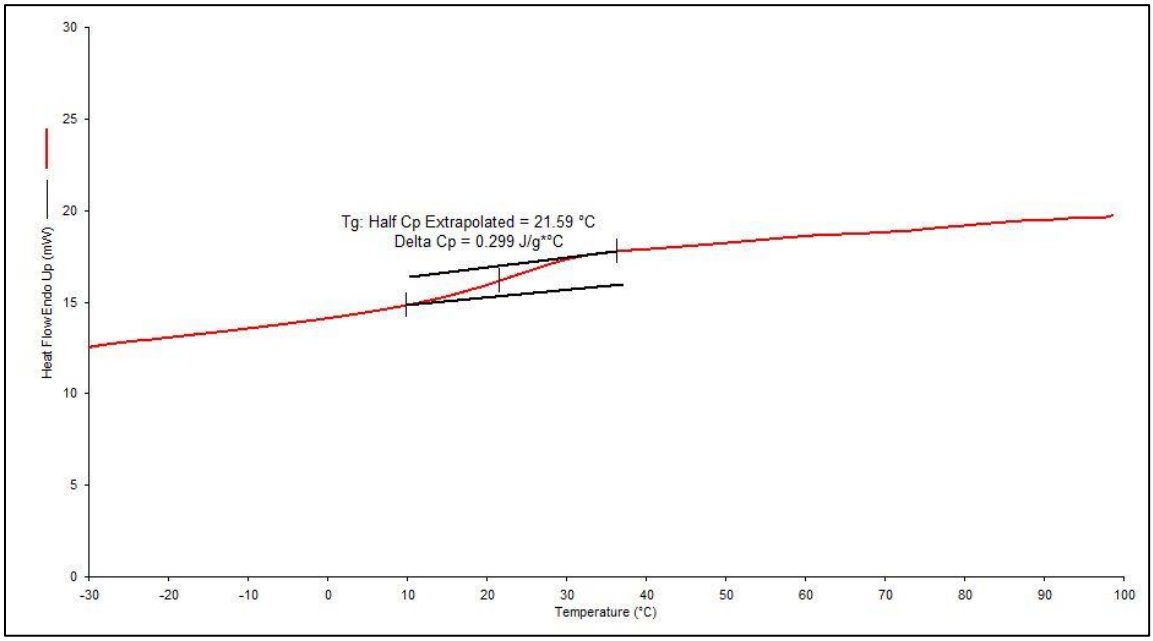

Figure S31. Glass transition temperature for polymer adhesive PA-4 at decrosslinked state.

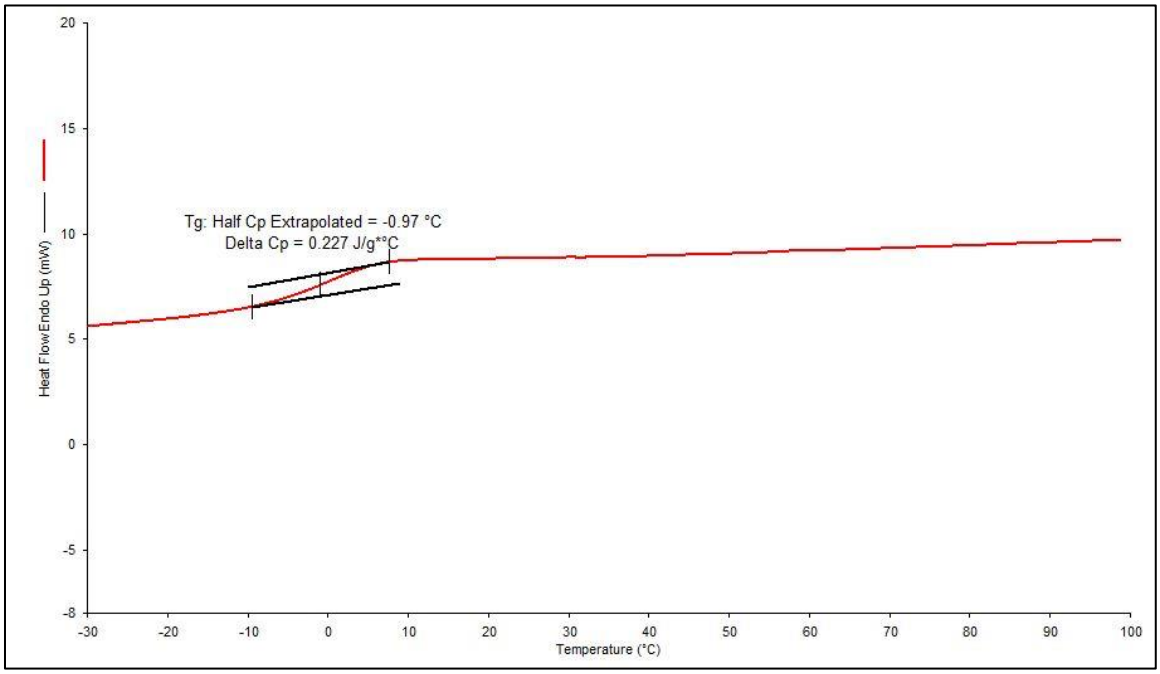

Figure S32. Glass transition temperature for polymer adhesive PA-5 at crosslinked state.

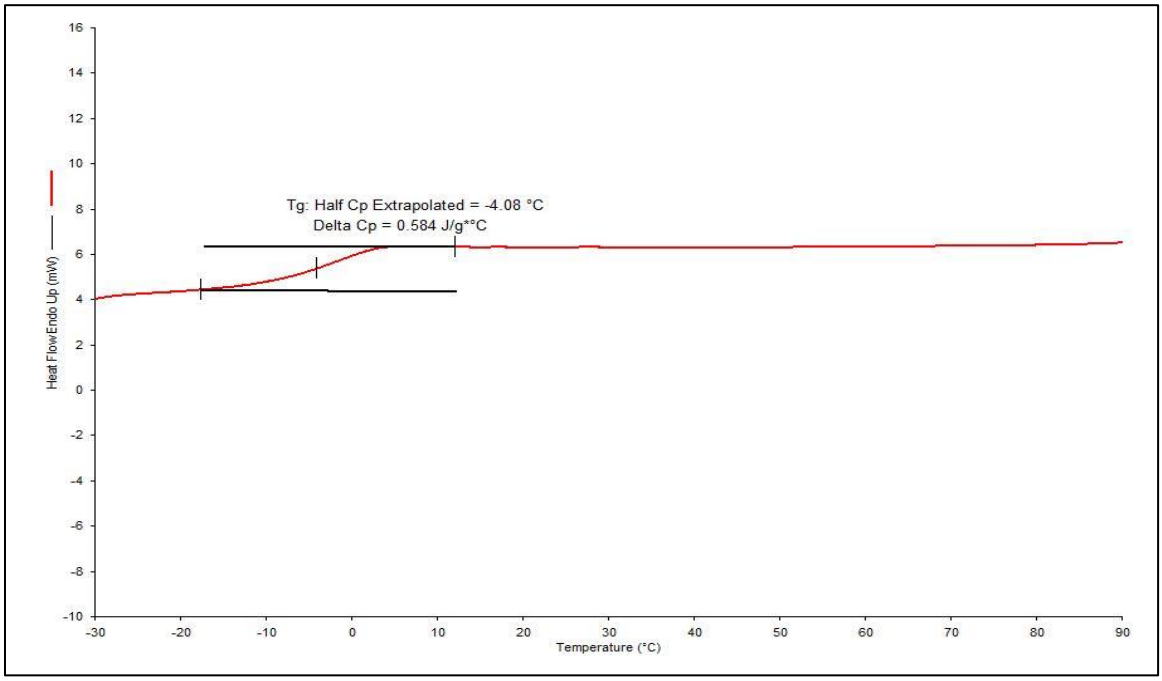

Figure S33. Glass transition temperature for polymer adhesive PA-5 at decrosslinked state.

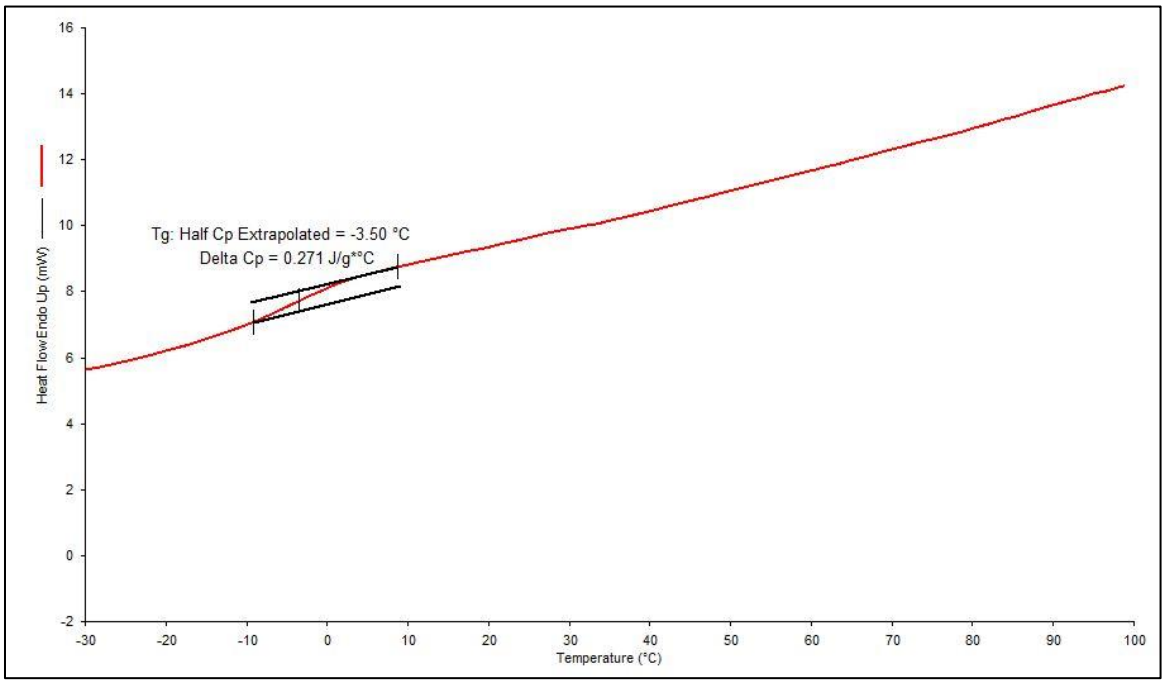

Figure S34. Glass transition temperature for polymer adhesive PA-6 at crosslinked state.

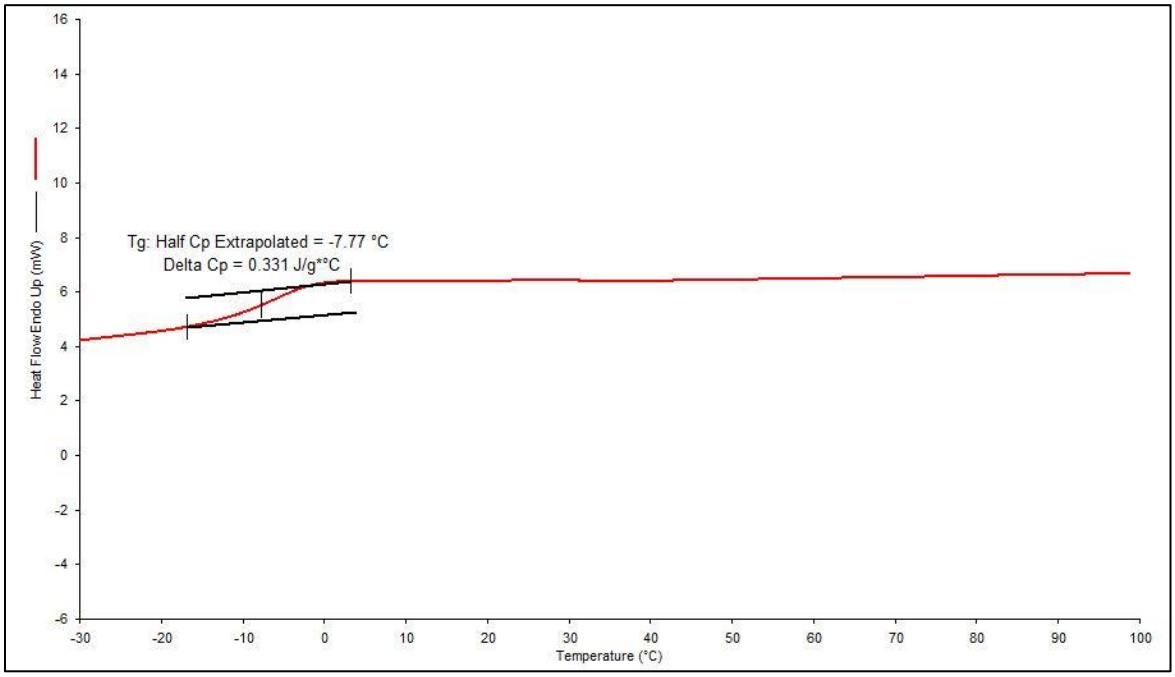

Figure S35. Glass transition temperature for polymer adhesive PA-6 at decrosslinked state.

6. Additional adhesive lap shear strength testing results for polymer adhesive PA-1

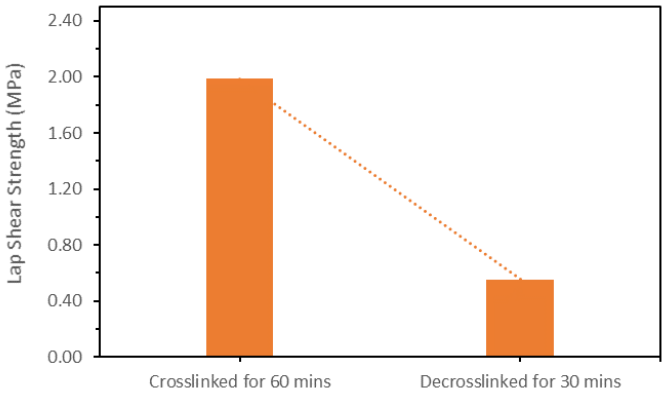

Figure S36. Reversibility test for the lap shear strength at 1.5 M concentration irradiated with 365 nm and 254 nm respectively.

7. Design of experiment

Table S1. Design of Experiments for the adhesive strength

Exp. No.	Exp. Name	Run Order	Incl/Excl	Molar Concentration (mol/L)	Irradiation Time (min)	Lap Shear Strength (MPa)
1	N1	1	Incl	0.125	5	0
2	N2	6	Incl	1	5	0.1
3	N3	7	Incl	0.125	120	0
4	N4	14	Incl	1	120	1.57

5	N5	5	Excl	0.125	43.3333	0[a]
6	N6	4	Excl	1	43.3333	0[a]
7	N7	11	Incl	1	81.6667	1.55
8	N8	8	Incl	0.416667	5	0.08
9	N9	9	Incl	0.708333	5	0.23
10	N10	10	Incl	0.708333	120	1.11
11	N11	2	Incl	0.5625	62.5	0.87
12	N12	12	Incl	0.5625	62.5	0.9
13	N13	13	Incl	0.5625	62.5	0.92
14	N14	3	Incl	0.5625	62.5	0.99

[a] abnormal value excluded of the DoE

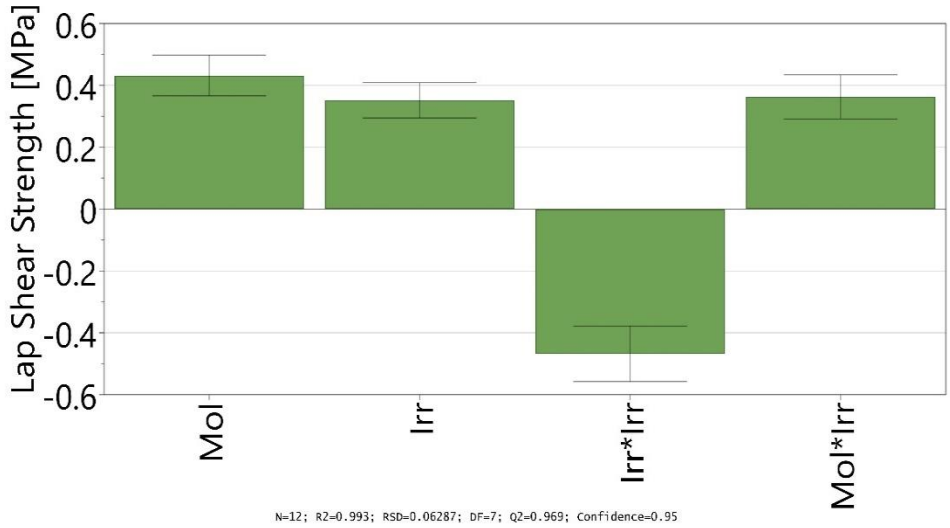

Figure S37. D-optimal coefficients of the quadratic model for the Lap Shear Strength.

Table S2. Analysis of variance (ANOVA) for the model.

Lap Shear Strength	Degrees of Freedom (DF)	Sum of Squares (SS)	Mean Squares (MS) Variance	F-Value	p-Value	Standard Deviation (SD)
Total	12	9.5622	0.79685			
Constant	1	5.76853	5.76853			
Total corrected	11	3.79367	0.344879			0.587264
Regression	4	3.766	0.9415	238.2	**0**[a]	0.970309
Residual	7	0.0276679	0.00395255			0.0628693

Lack of Fit (Model error)	4	0.0198679	0.00496697	1.91037	**0.311** [b]	0.0704767
Pure error (Replicate error)	3	0.0078	0.0026			0.0509902
	N = 12	Q^2 = 0.969		Cond. no. =	3.02	
	DF = 7	R^2 = 0.993		Relative Standard Deviation (RSD) =	0.06287	
		R^2 adj. [c] = 0.989				

[a] Significance of the model at 95% confidence level

[b] $p > 0.05$ no lack of fit

[c] R^2 adjusted for degree of freedom

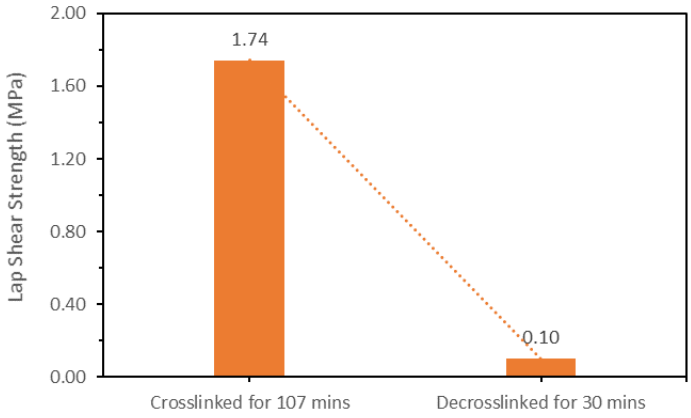

Figure S38. Reversibility test for the lap shear strength value at 1 M concentration irradiated with 365 nm and 254 nm respectively.

8. Optical microscope images for failure mode analysis

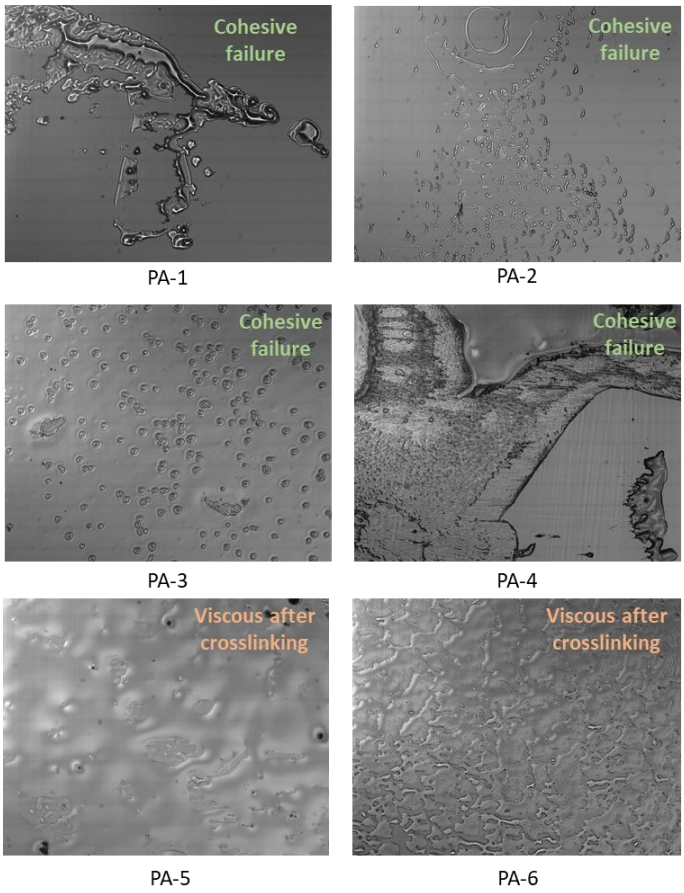

Figure S39. Failure analysis for all the polymer adhesive structures PA-1 to PA-6.